HHS Public Access

Author manuscript

ACS Sens. Author manuscript; available in PMC 2023 March 03.

Published in final edited form as:

ACS Sens. 2022 December 23; 7(12): 3644–3653. doi:10.1021/acssensors.2c01909.

Flexible and Implantable Polyimide Aptamer-Field-Effect Transistor Biosensors

Chuanzhen Zhao[1,2], **Tianxing Man**[3], **Yan Cao**[2,4], **Paul S. Weiss**[1,2,5], **Harold G. Monbouquette**[2,4], **Anne M. Andrews**[1,2,6,*]

[1]Department of Chemistry and Biochemistry, University of California, Los Angeles, Los Angeles, California 90095, United States

[2]California NanoSystems Institute, University of California, Los Angeles, Los Angeles, California 90095, United States

[3]Department of Mechanical and Aerospace Engineering, University of California, Los Angeles, Los Angeles, California 90095, United States

[4]Department of Chemical and Biomolecular Engineering, University of California, Los Angeles, Los Angeles, California 90095, United States

[5]Departments of Bioengineering and Materials Science and Engineering, University of California, Los Angeles, Los Angeles, California 90095, United States

[6]Department of Psychiatry and Biobehavioral Sciences, Semel Institute for Neuroscience & Human Behavior, and Hatos Center for Neuropharmacology, University of California, Los Angeles, Los Angeles, California 90095, United States

Abstract

Monitoring neurochemical signaling across timescales is critical to understanding how brains encode and store information. Flexible (*vs.* stiff) devices have been shown to improve *in vivo* monitoring, particularly over longer times, by reducing tissue damage and immunological responses. Here, we report our initial steps toward developing flexible and implantable neuroprobes with aptamer-field-effect transistor (FET) biosensors for neurotransmitter monitoring. A high-throughput process was developed to fabricate thin, flexible polyimide probes using micro-electro-mechanical-system (MEMS) technologies, where 150 flexible probes were fabricated on each 4-inch Si wafer. Probes were 150-μm wide and 7-μm thick with two FETs per tip. The bending stiffness was 1.2×10^{-11} N·m^2. Semiconductor thin films (3-nm In_2O_3) were

*To whom correspondence should be addressed to: aandrews@mednet.ucla.edu.

Author Contributions

CZ and AMA designed the experiments. CZ, TM, and YC designed and fabricated the flexible neuroprobes. CZ carried out the sensing experiments and data analysis. CZ and AMA wrote the manuscript with input from all authors.

ASSOCIATED CONTENT

Supporting Information Available: The following files are available free of charge. Supplemental information includes a cross-sectional schematic of the flexible neuroprobe fabrication process, calculations of bending stiffness, and the statistical summary. A supplemental movie showing the implantation of a flexible neuroprobe is also available.

PSW and AMA have filed a patent on stem-loop receptor-based field-effect devices for sensing in physiological salt concentrations, U.S. PCT/US2019/046891. AMA and CZ have filed a patent for a wearable aptamer field-effect transistor sensing system for noninvasive cortisol monitoring and a wearable system for stress sensing, U.S. Provisional Application No. 63/296,447.

functionalized with DNA aptamers for target recognition, which produces aptamer conformational rearrangements detected *via* changes in FET conductance. Flexible aptamer-FET neuroprobes detected serotonin at femtomolar concentrations in high-ionic strength artificial cerebrospinal fluid. A straightforward implantation process was developed, where micro-fabricated Si carrier devices assisted with implantation such that flexible neuroprobes detected physiological relevant serotonin in a tissue-hydrogel brain mimic.

Graphical Abstract

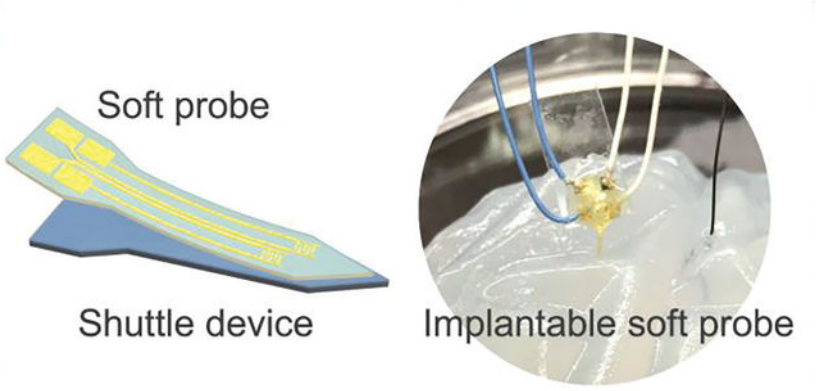

Keywords

Flexible electronics; biosensors; DNA; neurotransmitter; implantable device

Implantable bioelectronics are powerful tools to monitor neural activity.[1–4] Implanted devices enable new discoveries associated with understanding healthy brain function and the biological basis and treatment mechanisms of neurological and neuropsychiatric disorders.[5–10] Devices for monitoring *in vivo* electrical signals have been extensively developed enabling chronic recordings lasting over six months with single neuron resolution.[11–20] In addition to electrical signals, chemical communication *via* neurotransmitters plays a central role in brain information processing. However, existing device technologies for neurochemical recordings are more limited.[5,21–23] A major challenge in neurochemical sensing is the development of biosensors that can detect arrays of neurotransmitters *in vivo* with high sensitivity and selectivity.

Recently, we developed aptamer-field-effect transistor (FET) biosensors for neurotransmitter detection.[4,23–28] Thin films of biocompatible In_2O_3 (~3 nm) for signal transduction were functionalized with single-stranded DNA (aptamers) for target recognition.[24–26] Aptamers selected for specific targets were covalently coupled to semiconductor surfaces.[24] Upon target capture, negatively charged oligonucleotide backbones undergo conformational changes near FET surfaces resulting in measurable changes in FET conductance and hence, target-related current. This sensing mechanism is universal since it is independent of the charge or electrochemical properties of the analytes themselves.[24] We have shown that aptamer-FETs can be used to detect biomarkers, including serotonin, dopamine, glucose, the membrane lipid S-1-P, phenylalanine, and cortisol in complex physiological

environments.[24–27] Aptamer-FET biosensors show high selectivity to targets *vs.* structurally similar molecules. Recently, Zhang and coworkers developed graphene-based aptamer-FET biosensors using our aptamers for dopamine and serotonin sensing.[29,30]

To monitor neurotransmitters *in vivo*, we developed Si-based implantable neuroprobes with miniaturized aptamer-FET biosensors. Probes were either 150 μm or 50 μm in width and thickness at the tips.[4] The larger neuroprobes were implanted in awake, behaving mice where they detected electrically stimulated serotonin release with high sensitivity. While our previous study showed results for acute measurements (*i.e.*, hours), challenges remain for stable, chronic *in vivo* recordings.[31,32]

Conventional implantable electrodes, including the first-generation neuroprobes we developed, are typically fabricated using rigid substrates such as metals or Si, which are much stiffer than biological tissues.[33] For example, Si has a Young's modulus of ~200 GPa, while brain tissue has a Young's modulus of ~10 kPa. This Young's modulus mismatch of $>10^7$ induces immunological responses and subsequent glial scar formation. For biosensing applications, immunological responses lead to signal drift due to biofouling.[31,34] Scar formation decreases device recording accuracy and sensitivity over time.[31,34–38] Moreover, the formation of glial scars leads to biosensor failure due to limited access between the sensing surface and tissue interface.[34]

Recent developments in soft and flexible electronics show potential for overcoming these limitations.[14,20,22,39–45] Flexible bioelectronics with lower device Young's moduli (*i.e.*, increased elasticity) showed reduced immunological responses after brain implantation compared with rigid substrates.[31,34,43,46,47] Flexible devices with the capability to detect neurotransmitters in real time are necessary to understand chemical neurotransmission, particularly *via* chronic neural recordings.[4,21,30,35] Along these lines, we recently developed a wearable smartwatch for sweat cortisol sensing using flexible polyimide-based aptamer FETs.[28] We also fabricated In_2O_3 nanoribbon aptamer-FET biosensor arrays on flexible poly(ethylene terephthalate) (PET) for the multiplexed detection of serotonin, dopamine, pH, and temperature in real time.[26]

Many flexible substrates (*e.g.*, PET and polyimide) still have Young's moduli (typically on the order of GPa) that are orders of magnitude greater than brain tissue. One promising strategy to reduce the bending stiffness of a material is to reduce its thickness, as bending stiffness decreases cubically with thickness (equation shown in the Supporting Information).[48] Recently, polyimide devices with thicknesses <10 μm have been shown to have optimal bending stiffness and conformal contact with tissue.[20,40,42,49] However, ultrathin devices are difficult to process and handle.[30,40,50] Moreover, due to the low bending stiffness, thin flexible probes suffer from buckling during penetration into tissues, making them challenging to implant.

Here, we report on fabrication and implantation strategies for flexible and implantable polyimide (7-μm) aptamer-FET neuroprobes to monitor the small-molecule neurotransmitter serotonin. We designed a high-throughput process to fabricate polyimide neuroprobes using micro-electro-mechanical-system (MEMS) technologies, which are scalable, high

throughput, and compatible with other microfabrication processes.[4] Quasi-2D In_2O_3 FETs were fabricated on the probe tips. With aptamers functionalized on the In_2O_3 surfaces, flexible neuroprobes were used to detect serotonin at femtomolar concentrations in artificial cerebrospinal fluid (aCSF). We used an artificial brain tissue matrix to develop and to test a process to implant flexible probes using a rigid carrier as a temporary shuttle device with straightforward probe release. Flexible aptamer-FET probes were implanted into a brain-tissue hydrogel mimic and showed high sensitivities to serotonin.

Experimental Section

Materials

Oligonucleotides (aptamers) were obtained from Integrated DNA Technologies (Coralville, IA). The SYLGARD 184 used to make polydimethylsiloxane (PDMS) wells for recordings was from Dow Corning Corporation (Midland, MI). Deionized water (18.2 MΩ) was dispensed *via* a Milli-Q system (Millipore, Billerica, MA). Polyimide solution (#PI-2611) was provided by Dupont Teijin Films (Chester, VA). Prime quality 4-inch Si wafers (P/B, thickness 500 μm and 150 μm) were purchased from Silicon Valley Microelectronics, Inc. (Santa Clara, CA, USA). All other materials were purchased from Sigma-Aldrich Co. (St. Louis, MO) unless otherwise noted.

Neuroprobe fabrication

Polyimide solutions were spin-coated at 3000 rpm for 30 s onto 500 μm thick Si wafers to form a 7-μm thick film, as reported previously.[28] After coating, substrates were pre-heated at 90 °C for 90 s and then at 150 °C for 90 s on a hot plate. Afterward, the substrates were transferred to an oven and annealed at 350 °C for 30 min. Aqueous solutions (0.1 M) of indium(III) nitrate hydrate (99.999%) were then spin-coated at 3000 rpm for 30 s onto polyimide-coated Si wafers. After deposition of indium precursors, substrates were heated to 150 °C for 10 min, followed by 3 h of annealing at 350 °C.[23,51] Source and drain electrodes (10 nm Ti and 30 nm Au) were deposited by electron-beam evaporation (CHA Industries, Inc., Fremont, CA) and patterned *via* standard photolithography. A second photolithographic process was performed to define the outer perimeter of the probes. Reactive ion etching was used to etch through the polyimide substrates using a plasma etching system (STS-AOE, Plasmatreat, Hayward, CA) with the protection of the photoresist. Probes were released from carrier wafers using tweezers. The source and drain electrodes of the neuroprobes were connected with wiring using Ag epoxy (Ted Pella, Redding, CA).[4]

Implantation of flexible neuroprobes

Shuttle devices were fabricated from Si using previously published methods.[4] Briefly, Si substrates (150 μm thick) were coated with photoresist to define probe profiles. Deep reactive ion etching using the Bosch process was used to etch through the unmasked regions of the silicon substrates using a Deep Silicon Etcher III (Plasma-Therm, Fremont, CA). To attach the flexible polyimide probes, Si shuttles were immersed into a physiological buffer solution to form a thin solution film on the Si surfaces. Since probes are destined for eventual brain implantation, we used aCSF as the buffer. Detailed aCSF preparation protocols are described in our previous work.[27] The polyimide probes were then attached

to the Si shuttles *via* capillary forces. Alignment between polyimide probes and Si shuttle devices was achieved using tweezers under an optical microscope (Figure 3c).

To mimic the properties of brain tissue for implantation, we used a 0.6% (w/v) agarose hydrogel, which was prepared by mixing agarose powder and aCSF. The mixture was microwaved until the agarose powder was dissolved (~1 min), poured into a container, and cooled to room temperature. Assembled probes and shuttles were implanted into the brain-mimic hydrogel using tweezers. After implantation for ~1 min, the Si shuttle devices were removed from the hydrogel leaving the polyimide probes in place (Movie S1).

In vitro experiments

To test device biosensing capabilities *in vitro*, we rinsed the FET probes in ethanol and dried with N_2 immediately before functionalization with thiolated serotonin aptamers. Mixtures of (3-aminopropyl)triethoxysilane and trimethoxy(propyl)silane (1:9, v/v) were thermally deposited on In_2O_3 at 40 °C for 1 h and annealed at 60 °C for 10 min.[4,23,24] Source and drain electrodes were insulated with a self-assembled monolayer of 1-dodecanethiol by immersing in 1 mM ethanolic solutions for 1 h. Probes were then immersed in 1 mM 3-maleimidobenzoic acid *N*-hydroxysuccinimide ester dissolved in 1:9 (v/v) mixture dimethyl sulfoxide and phosphate-buffered saline (PBS, Gibco, Fisher Scientific, Waltham, MA) for 30 min. To immobilize aptamers, probes were immersed in a 1 μM solution of thiolated DNA in PBS overnight. Probes were rinsed with deionized water and dried with N_2 before measurements. *In vitro* testing was performed by adding different concentrations of serotonin into aCSF in PDMS wells sealed to each device.

Ex vivo experiments

Brain tissue lacking serotonin was obtained from *Tph2* knockout mice.[52] Mice were exsanguinated by cardiac perfusion and brains were cleared of blood containing serotonin synthesized by peripheral *Tph1*. The brains were then shipped to UCLA on dry ice from the laboratory of Dr. Donald Kuhn (Wayne State University, Detroit, MI). Brain tissue was stored at -80 °C until use. Brain tissue collection procedures were approved by the Wayne State University Institutional Animal Care and Use Committee.

Brain tissue was homogenized in ice-cold aCSF (1:1 w/v) using a VirTis Virsonic600 ultrasonic cell disruptor (Gardiner, NY) with the microtip set at 4 and a 50% duty cycle for 30–40 pulses/s. Homogenized brain tissue solutions were mixed with agarose powder and aCSF to make 0.6% agarose gels. The mixture was microwaved just until the agarose powder dissolved (~1 min, melting point of ~65 °C). The solution was poured into a brain mold to mimic brain cortical morphology and immediately cooled. Flexible neuroprobes were implanted into the brain tissue hydrogel using the method described above. A Ag/AgCl gate electrode, constructed from a 0.010-inch diameter Ag wire freshly coated with AgCl (A-M Systems, Sequim, WA) by immersing in a bleach solution (Clorox, Oakland, California) for 5 min, was implanted into the brain tissue hydrogel next to the probe. A 2-μL aliquot of 50 μM serotonin was injected into the hydrogel (~0.2 cm away from the probe tip) for a final serotonin concentration of 100 nM (calculated based on 100-mL aCSF in the hydrogel).

All FET measurements were performed using a Keithley 4200A SCS semiconductor analyzer (Tektronix, Beaverton, OR). Source-drain current (I_{DS}) transfer curves were obtained by sweeping the gate voltage (V_{GS}) from 100 to 350 mV while maintaining the drain voltage (V_{DS}) at 10 mV, which took ~5 s for each scan. Calibrated responses were calculated at 300 mV to minimize device-to-device variation, as previously described.[24,53]

Statistics

Data from FET calibrated responses are reported as means ± standard errors of the means and were analyzed using GraphPad Prism 7.04 (GraphPad Software Inc., San Diego, CA) *via* one-way analysis of variance followed by Tukey's multiple comparisons *post hoc* tests with repeated measures.

RESULTS AND DISCUSSION

The process used to fabricate flexible In_2O_3 FET neuroprobes is described in detail in the Experimental Section and illustrated in Figure 1 and Figure S1. We leveraged our earlier high-throughput fabrication process for 150-μm and 50-μm Si neuroprobes using MEMS technologies.[4] Polyimide (~7-μm) and In_2O_3 (~3-nm) films were fabricated sequentially on Si substrates using solution processing, followed by photolithography to define the Au and Ti source and drain electrodes. A layer of parylene can be added to the probe shafts to isulate source/drain interconnects, as demonstrated by us previously.[4] Probe outlines were also defined photolithographically. We used In_2O_3 as the semiconductor due to its straightforward sol-gel fabrication. Others have shown that In_2O_3 is more stable than other metal oxides (*e.g.*, indium-gallium-zinc oxide (IGZO)) in physiological electrolyte solutions.[23,54] The thickness of In_2O_3 on polyimide (3 nm) was determined by atomic force microscopy, as shown in our previous work.[28]

This fabrication process is high throughput and scalable such that 150 probes were fabricated per 4" wafer (Figure 2a). Probes were delaminated from Si substrates using tweezers to produce free-standing devices. A delaminated probe is shown in Figure 2b, leaving an outline of the probe on the wafer. The freestanding polyimide probes are flexible and make conformal contact with the convoluted surface of an agarose hydrogel brain model (Figure 2c). Each probe was ~7 μm thick and ~150 μm wide with two FETs side-by-side on the tip (Figure 2d).

The bending stiffness of these polyimide probes is 1.2×10^{-11} N·m^2, which is seven orders of magnitude lower than that of the smallest optical fibers (230-μm-outer diameter polyethylene fibers with silica cores, 1×10^{-5} N·m^2, calculations shown in the Supporting Information).[30,55] The effective bending stiffness of the polyimide probes (bending stiffness per width) is ~8×10^{-8} N·m, which is less than that of commonly used soft elastomers, *e.g.,* polydimethylsiloxane (2.2×10^{-7} N·m at 100 μm thickness).[56] Previous histological studies have shown that polyimide devices of similar thickness and bending stiffness induce minimal immune responses.[30,40] Note that the width of the probes and FETs can be scaled down in a straightforward manner to 50 μm using photolithography, as we have previously demonstrated using Si as the device substrate.[4] Polyimide is thermally stable and compatible with most microfabrication processes up to 350 °C. Previously, we showed that

the electronic and biosensing performance of In_2O_3 FETs on polyimide remains stable even after 100 bending cycles.[28] This straightforward and universal fabrication strategy opens opportunities to integrate polyimide neuroprobes with other neural recording and modulating modalities on a single flexible platform, *e.g.*, electrophysiology and optical stimulation capabilities.

A Ag/AgCl electrode was used to gate thin-film In_2O_3 FETs on flexible neuroprobes through the buffer solution, where electrical double layers were used as the gate dielectric (Figure 2e). Source and drain electrodes were connected to the semiconductor analyzer *via* copper wiring to apply voltages to the interdigitated electrodes covered by a buffer solution.[4] For serotonin sensing, the In_2O_3 surface was covalently functionalized with serotonin aptamers.[24] The detailed functionalization process is described in the Experimental Section and depicted in Figure 2f. Here, self-assembled monolayers on the Au source and drain electrodes combined with the electrical double layers in the buffer solution serve as capacitors for insulation.[24,27] Typical transistor performance was observed from the FETs in aCSF, with transfer and output characteristics shown in Figure 2g and 2h, respectively.

Serotonin was introduced to sensors to test responses. We used aCSF to mimic the ionic strength of the extracellular space in brain tissue. The FETs on flexible probes responded to serotonin in the pM to μM range covering the physiological range of serotonin in the brain extracellular space,[57–60] as highlighted in yellow in Figure 2i. The serotonin aptamer used here was previously demonstrated to be highly selective for serotonin *vs.* interfering molecules (*i.e.*, L-5-hydroxytryptophan, 5-hydroxyindoleacetic acid, dopamine, L-tryptophan, uric acid, and ascorbic acid) when tested on FETs on Si.[4,24] We expect similar selectivity for the flexible polyimide neuroprobes since only the substrate was changed; we used the same aptamer to detect serotonin.

To monitor serotonin *in vivo*, neuroprobes need to be implanted into different areas of the brain where serotonin cell bodies and axons are found.[57] However, the softness of the polyimide probes leads to bunching during tissue penetration.[3,32] There have been several strategies developed to assist in the implantation of soft probes, including coating probes with a stiffening polymer, rapid freezing, or using liquid metal or temperature-adaptive Young's moduli systems.[42,47,50,61–63] However, current implantation strategies typically require re-engineering of device architectures or complicated assembly processes. Moreover, since biosensor surfaces are usually functionalized with receptors, *e.g.*, antibodies or aptamers, before the implantation process, implantation strategies should not damage the functionalized layer.

Here, we developed a one-step shuttle-assisted process for flexible neuroprobe implantation using surface tension. As shown in Figure 3a, a Si shuttle was fabricated to have the same lateral dimensions as the flexible neuroprobes (150 μm). Fabrication was the same as described in our previous work[4] and in the Experimental Section. The similar shapes of the Si shuttle device and the flexible polyimide neuroprobes minimized tissue damage from the shuttle device during the penetration process. The Si shuttle device was treated with O_2 plasma to make it hydrophilic before dipping into the buffer solution (*i.e.*, aCSF). The thin layer of buffer coating the Si shuttle surface was used to affix a flexible neuroprobe *via*

van der Waals forces. The neuroprobe and shuttle were aligned under an optical microscope using tweezers (Figure 3b).

After assembly, the shuttle+neuroprobe was implanted. To mimic brain tissue, we used a 0.6% agarose hydrogel with aCSF, which closely resembles several critical physical characteristics of brain tissue, including the penetration force.[47,64] After inserting the assembled device into the brain-mimic, the buffer layer between the flexible neuroprobe and shuttle device diffused into the hydrogel, reducing the surface tension holding the two parts together. The shuttle device was then retracted leaving the flexible device in place in the hydrogel (Figure 3b–f, Movie S1). During the removal of the shuttle device, we did not observe movement of the flexible probe, as shown in the movie (Movie S1). For future *in vivo* experiments, it would be necessary to investigate further the accuracy of positioning during the implantation processes.

Sensing *in vivo* entails detecting specific targets in complex biological matrices containing a wide range of neurotransmitters (nontargets), metabolites and other interferants, and biomacromolecules (biofouling). To investigate the sensing capabilities of the flexible neuroprobes in a biological matrix that more closely approximates an *in vivo* environment, we used brain tissue from *Tph2*-null mice.[4] These mice do not express the rate-limiting serotonin synthetic enzyme in the central nervous system (CNS), and thus lack endogenous brain serotonin (Figure 4a).

Brain tissue homogenates from *Tph2*-null mice were incorporated into 0.6% agarose hydrogel in aCSF. As such, we produced an *ex vivo* model that mimicked the ionic strength of the extracellular space and approximated the chemical and physical properties of the *in vivo* brain environment. Using brain tissue that lacks serotonin prevented swamping the FET sensors with high concentrations of endogenous intracellular stores of serotonin liberated during tissue homogenization. *In vivo*, FET sensors would not encounter vesicular serotonin except briefly during implantation.

This type of brain phantom mainly mimics the physical characteristics of the brain (*e.g.*, Young's modulus and penetration force) and ionic strength of the extracellular space in the brain.[47,64] The brain tissue in the agarose gel introduces biomolecules found in the *in vivo* environment. Nonetheless, the preparation process may affect the molecular composition originally present in the brain. Previously, we tested similar biosensors on Si substrates in fresh brain tissue containing endogenous small molecules and macromolecules. In both cases, aptamer-FET sensors showed high target sensitivity and low biofouling.[4,24]

Figure 4b and 4c, depict implantation of a representative flexible neuroprobe into a brain mimic using a Si shuttle, as described above. A Ag/AgCl electrode was then implanted to apply gate voltages through the hydrogel matrix (Figure 4b). We characterized the transistor performance of the flexible neuroprobes in this tissue-hydrogel phantom. As shown in Figure 4d and 4e, an implanted neuroprobe showed typical transfer and output characteristics with gate voltage and source-drain voltage modulation.

To simulate neurotransmitter release and diffusion in the brain, we used a syringe to inject 50 μM serotonin into the hydrogel. The recording sites were approximately 2 mm

away from the implanted neuroprobes. The final concentration (100 nM) was selected as a physiologically relevant serotonin concentration.[57–60] Data were collected before the introduction of serotonin and at different time intervals after its introduction. As shown in Figure 4g, five consecutive transfer curves overlapped with each other in the tissue-hydrogel brain-mimic, illustrating that the flexible neuroprobes were stable in the matrix without detectable signal drift prior to injection.

We observed significant increases in the responses of two different neuroprobes as early as 5 min after serotonin addition (see Table S1 for statistics). These data demonstrate that the flexible aptamer-FET neuroprobes detected diffusion-related changes in serotonin levels. We previously found that the response times of our aptamer-FET sensors are on the order of seconds;[26] the 5-min delay in response time here is due to target diffusion over ~2 mm in the hydrogel matrix from the introduction location to the recording site, which is similar to what we observed in a previous study using Si neuroprobes.[4] These findings illustrate that our flexible neuroprobes can be implanted into a solid matrix that mimics the rigidity and chemical composition of brain tissue to monitor physiologically relevant serotonin release.

CONCLUSIONS

We developed flexible and implantable neurochemical probes based on aptamer FET biosensors. A high-throughput fabrication strategy was developed to fabricate In_2O_3 thin-film (~3 nm) field-effect transistors on polyimide (7 μM) with up to 150 flexible neuroprobes on a 4-inch Si substrate. Flexible aptamer-FET neuroprobes detected serotonin down to femtomolar concentrations in artificial cerebrospinal fluid. To facilitate the implantation of these flexible devices, we developed a straightforward process where a rigid Si carrier device was used to assist in tissue penetration. To test the functionality of the flexible neuroprobes for future *in vivo* studies, we developed a brain phantom as an *ex vivo* model. We used agarose gel to mimic critical physical characteristics of the brain and aCSF to mimic the ionic strength of the brain's extracellular space. Moreover, we combined agarose gel with mouse brain tissue containing interferants and biomacromolecules present in the brain. The brain tissue phantom served as a model to evaluate sensor performance towards *in vivo* applications for neurochemical sensing. We showed that the flexible neuroprobes were stable while implanted in the hydrogel matrices with reproducible transistor performance and without short-term biofouling. We were able to detect serotonin injected into the brain tissue phantom suggesting the potential to monitor changes in serotonin levels *in vivo*.

While soft neuroprobes remain an important goal for tissue-like implantable bioelectronics, a longstanding question remains as to how soft and flexible is *soft and flexible enough* such that immunological responses are minimized? This issue is a grand challenge to the bioelectronics community that needs to be addressed and requires further study. Future histological studies as a function of implantation duration involving flexible *vs.* stiff probes will provide comparative information on immunological responses. Another key question involves the impact of device dimensions. Smaller implanted devices appear to reduce immune responses.[31,32,34] However, understanding how immunological responses change systematically in response to miniaturization is still unclear. Along these lines, we have

previously fabricated Si neuroprobes with 50-μm widths and thicknesses to compare with 150-μm neuroprobes in terms of tissue response. Scaling down the flexible neuroprobes developed in this work can be achieved using a similarly straightforward approach. Further histological studies comparing our devices of different sizes and stiffness are ongoing.

In addition to FETs, aptamers can be coupled with redox reporters for electrochemical sensing. For example, electrochemical aptamer-based (EAB) sensors have been used to track plasma drug concentrations in real-time.[65,66] Recently, a dopamine aptamer was coupled with carbon-fiber microelectrodes noncovalently or using an electrochemical conjugation strategy for dopamine sensing *in vivo* using cyclic voltammetry.[67,68] We envision that next-generation neuroprobes will need to be soft, multi-modal (*i.e.,* sense multiple neurotransmitters and electrophysiological signals, produce optical or electrical stimulation, and drug delivery all on the same device), and have long-term recording capabilities *in vivo*. Soft bioelectronics with the capability to detect multiple neurotransmitters simultaneously in real-time are needed to investigate chemical information processing in the brain, particularly in the context of chronic neural recordings during behavior.[21]

Supplementary Material

Refer to Web version on PubMed Central for supplementary material.

ACKNOWLEDGMENTS

This research was supported by funding from the National Institute on Drug Abuse (DA045550). We thank D. Kuhn (Wayne State University, Detroit, MI) for providing the *Tph2* knockout mouse brains. We thank HD Microsystems at Dupont (Wilmington, DE) for the polyimide solution (PI-2611). We acknowledge the facilities and thank the staff of the UCLA Nanolab. We thank Dr. Kevin M. Cheung and Dr. Jeffrey J. Schwartz for feedback on the manuscript. We thank Dr. Wenfei Liu and Dr. I-Wen Huang for technical assistance on device fabrication and functionalization. The illustration in Figure 4a was created using BioRender (biorender.com).

References

1. Seymour JP; Wu F; Wise KD; Yoon E State-of-the-Art MEMS and Microsystem Tools for Brain Research. Microsyst. Nanoeng. 2017, 3, 16066. [PubMed: 31057845]
2. Won SM; Song E; Zhao J; Li J; Rivnay J; Rogers JA Recent Advances in Materials, Devices, and Systems for Neural Interfaces. Adv. Mater. 2018, 30, e1800534. [PubMed: 29855089]
3. Woods GA; Rommelfanger NJ; Hong G Bioinspired Materials for in Vivo Bioelectronic Neural Interfaces. Matter 2020, 3, 1087–1113. [PubMed: 33103115]
4. Zhao C; Cheung KM; Huang IW; Yang H; Nakatsuka N; Liu W; Cao Y; Man T; Weiss PS; Monbouquette HG; Andrews AM Implantable Aptamer-Field-Effect Transistor Neuroprobes for *in Vivo* Neurotransmitter Monitoring. Sci. Adv. 2021, 7, eabj7422. [PubMed: 34818033]
5. Alivisatos AP; Andrews AM; Boyden ES; Chun M; Church GM; Deisseroth K; Donoghue JP; Fraser SE; Lippincott-Schwartz J; Looger LL; Masmanidis S; McEuen PL; Nurmikko AV; Park H; Peterka DS; Reid C; Roukes ML; Scherer A; Schnitzer M; Sejnowski TJ; et al. Nanotools for Neuroscience and Brain Activity Mapping. ACS Nano 2013, 7, 1850–1866. [PubMed: 23514423]
6. Altieri SC; Yang H; O'Brien HJ; Redwine HM; Senturk D; Hensler JG; Andrews AM Perinatal Vs Genetic Programming of Serotonin States Associated with Anxiety. Neuropsychopharmacology 2015, 40, 1456–1470. [PubMed: 25523893]
7. Malvaez M; Shieh C; Murphy MD; Greenfield VY; Wassum KM Distinct Cortical-Amygdala Projections Drive Reward Value Encoding and Retrieval. Nat. Neurosci. 2019, 22, 762–769. [PubMed: 30962632]

8. Dolensek N; Gehrlach DA; Klein AS; Gogolla N Facial Expressions of Emotion States and Their Neuronal Correlates in Mice. Science 2020, 368, 89–94. [PubMed: 32241948]

9. Lee K; Claar LD; Hachisuka A; Bakhurin KI; Nguyen J; Trott JM; Gill JL; Masmanidis SC Temporally Restricted Dopaminergic Control of Reward-Conditioned Movements. Nat. Neurosci. 2020, 23, 209–216. [PubMed: 31932769]

10. Topalovic U; Aghajan ZM; Villaroman D; Hiller S; Christov-Moore L; Wishard TJ; Stangl M; Hasulak NR; Inman CS; Fields TA; Rao VR; Eliashiv D; Fried I; Suthana N Wireless Programmable Recording and Stimulation of Deep Brain Activity in Freely Moving Humans. Neuron 2020, 108, 322–334. [PubMed: 32946744]

11. Chen R; Canales A; Anikeeva P Neural Recording and Modulation Technologies. Nat. Rev. Mater. 2017, 2, 16093. [PubMed: 31448131]

12. Ferro MD; Melosh NA Electronic and Ionic Materials for Neurointerfaces. Adv. Funct. Mater. 2018, 28, 1704335.

13. Viventi J; Kim DH; Vigeland L; Frechette ES; Blanco JA; Kim YS; Avrin AE; Tiruvadi VR; Hwang SW; Vanleer AC; Wulsin DF; Davis K; Gelber CE; Palmer L; Van der Spiegel J; Wu J; Xiao J; Huang Y; Contreras D; Rogers JA; et al. Flexible, Foldable, Actively Multiplexed, High-Density Electrode Array for Mapping Brain Activity in vivo. Nat. Neurosci. 2011, 14, 1599–1605. [PubMed: 22081157]

14. Vachicouras N; Tarabichi O; Kanumuri VV; Tringides CM; Macron J; Fallegger F; Thenaisie Y; Epprecht L; McInturff S; Qureshi AA; Paggi V; Kuklinski MW; Brown MC; Lee DJ; Lacour SP Microstructured Thin-Film Electrode Technology Enables Proof of Concept of Scalable, Soft Auditory Brainstem Implants. Sci. Transl. Med. 2019, 11, eaax9487. [PubMed: 31619546]

15. Du J; Blanche TJ; Harrison RR; Lester HA; Masmanidis SC Multiplexed, High Density Electrophysiology with Nanofabricated Neural Probes. PLoS One 2011, 6, e26204. [PubMed: 22022568]

16. Rios G; Lubenov EV; Chi D; Roukes ML; Siapas AG Nanofabricated Neural Probes for Dense 3-D Recordings of Brain Activity. Nano Lett. 2016, 16, 6857–6862. [PubMed: 27766885]

17. Jun JJ; Steinmetz NA; Siegle JH; Denman DJ; Bauza M; Barbarits B; Lee AK; Anastassiou CA; Andrei A; Aydin C; Barbic M; Blanche TJ; Bonin V; Couto J; Dutta B; Gratiy SL; Gutnisky DA; Hausser M; Karsh B; Ledochowitsch P; et al. Fully Integrated Silicon Probes for High-Density Recording of Neural Activity. Nature 2017, 551, 232–236. [PubMed: 29120427]

18. Driscoll N; Richardson AG; Maleski K; Anasori B; Adewole O; Lelyukh P; Escobedo L; Cullen DK; Lucas TH; Gogotsi Y; Vitale F Two-Dimensional Ti3C2 MXene for High-Resolution Neural Interfaces. ACS Nano 2018, 12, 10419–10429. [PubMed: 30207690]

19. Jiang Y; Li X; Liu B; Yi J; Fang Y; Shi F; Gao X; Sudzilovsky E; Parameswaran R; Koehler K; Nair V; Yue J; Guo K; Tsai H-M; Freyermuth G; Wong RCS; Kao C-M; Chen C-T; Nicholls AW; Wu X; et al. Rational Design of Silicon Structures for Optically Controlled Multiscale Biointerfaces. Nat. Biomed. Eng. 2018, 2, 508–521. [PubMed: 30906646]

20. He F; Sullender CT; Zhu H; Williamson MR; Li X; Zhao Z; Jones TA; Xie C; Dunn AK; Luan L Multimodal Mapping of Neural Activity and Cerebral Blood Flow Reveals Long-Lasting Neurovascular Dissociations after Small-Scale Strokes. Sci. Adv. 2020, 6, eaba1933. [PubMed: 32494746]

21. Andrews AM The Brain Initiative: Toward a Chemical Connectome. ACS Chem. Neurosci. 2013, 4, 645. [PubMed: 23862750]

22. Li J; Liu Y; Yuan L; Zhang B; Bishop ES; Wang K; Tang J; Zheng YQ; Xu W; Niu S; Beker L; Li TL; Chen G; Diyaolu M; Thomas AL; Mottini V; Tok JB; Dunn JCY; Cui B; Pasca SP; et al. A Tissue-Like Neurotransmitter Sensor for the Brain and Gut. Nature 2022, 606, 94–101. [PubMed: 35650358]

23. Kim J; Rim YS; Chen H; Cao HH; Nakatsuka N; Hinton HL; Zhao C; Andrews AM; Yang Y; Weiss PS Fabrication of High-Performance Ultrathin In2O3 Film Field-Effect Transistors and Biosensors Using Chemical Lift-Off Lithography. ACS Nano 2015, 9, 4572–4582. [PubMed: 25798751]

24. Nakatsuka N; Yang KA; Abendroth JM; Cheung KM; Xu X; Yang H; Zhao C; Zhu B; Rim YS; Yang Y; Weiss PS; Stojanovic MN; Andrews AM Aptamer-Field-Effect Transistors Overcome

Debye Length Limitations for Small-Molecule Sensing. Science 2018, 362, 319–324. [PubMed: 30190311]

25. Cheung KM; Yang KA; Nakatsuka N; Zhao C; Ye M; Jung ME; Yang H; Weiss PS; Stojanovic MN; Andrews AM Phenylalanine Monitoring via Aptamer-Field-Effect Transistor Sensors. ACS Sens. 2019, 4, 3308–3317. [PubMed: 31631652]
26. Liu Q; Zhao C; Chen M; Liu Y; Zhao Z; Wu F; Li Z; Weiss PS; Andrews AM; Zhou C Flexible Multiplexed In2O3 Nanoribbon Aptamer-Field-Effect Transistors for Biosensing. iScience 2020, 23, 101469. [PubMed: 33083757]
27. Zhao C; Liu Q; Cheung KM; Liu W; Yang Q; Xu X; Man T; Weiss PS; Zhou C; Andrews AM Narrower Nanoribbon Biosensors Fabricated by Chemical Lift-Off Lithography Show Higher Sensitivity. ACS Nano 2021, 15, 904–915. [PubMed: 33337135]
28. Wang B; Zhao C; Wang Z; Yang KA; Cheng X; Liu W; Yu W; Lin S; Zhao Y; Cheung KM; Lin H; Hojaiji H; Weiss PS; Stojanovic MN; Tomiyama AJ; Andrews AM; Emaminejad S Wearable Aptamer-Field-Effect Transistor Sensing System for Noninvasive Cortisol Monitoring. Sci. Adv. 2022, 8, eabk0967. [PubMed: 34985954]
29. Gao Z; Wu G; Song Y; Li H; Zhang Y; Schneider MJ; Qiang Y; Kaszas J; Weng Z; Sun H; Huey BD; Lai RY; Zhang Y Multiplexed Monitoring of Neurochemicals via Electrografting-Enabled Site-Selective Functionalization of Aptamers on Field-Effect Transistors. Anal. Chem. 2022, 94, 8605–8617. [PubMed: 35678711]
30. Wu G; Zhang N; Matarasso A; Heck I; Li H; Lu W; Phaup JG; Schneider MJ; Wu Y; Weng Z; Sun H; Gao Z; Zhang X; Sandberg SG; Parvin D; Seaholm E; Islam SK; Wang X; Phillips PEM; Castro DC; et al. Implantable Aptamer-Graphene Microtransistors for Real-Time Monitoring of Neurochemical Release in Vivo Nano Lett. 2022, 22, 3668–3677. [PubMed: 35439419]
31. Salatino JW; Ludwig KA; Kozai TDY; Purcell EK Glial Responses to Implanted Electrodes in the Brain. Nat. Biomed. Eng. 2017, 1, 862–877. [PubMed: 30505625]
32. Chen Y; Rommelfanger NJ; Mahdi AI; Wu X; Keene ST; Obaid A; Salleo A; Wang H; Hong G How Is Flexible Electronics Advancing Neuroscience Research? Biomaterials 2021, 268, 120559. [PubMed: 33310538]
33. Wassum KM; Tolosa VM; Wang J; Walker E; Monbouquette HG; Maidment NT Silicon Wafer-Based Platinum Microelectrode Array Biosensor for Near Real-Time Measurement of Glutamate in Vivo. Sensors (Basel) 2008, 8, 5023–5036. [PubMed: 19543440]
34. Kozai TD; Jaquins-Gerstl AS; Vazquez AL; Michael AC; Cui XT Brain Tissue Responses to Neural Implants Impact Signal Sensitivity and Intervention Strategies. ACS Chem. Neurosci. 2015, 6, 48–67. [PubMed: 25546652]
35. Du ZJ; Kolarcik CL; Kozai TDY; Luebben SD; Sapp SA; Zheng XS; Nabity JA; Cui XT Ultrasoft Microwire Neural Electrodes Improve Chronic Tissue Integration. Acta Biomater. 2017, 53, 46–58. [PubMed: 28185910]
36. Schwartz AB Cortical Neural Prosthetics. Annu. Rev. Neurosci. 2004, 27, 487–507. [PubMed: 15217341]
37. Kozai TDY; Vazquez AL; Weaver CL; Kim S-G; Cui XT *In vivo* Two-Photon Microscopy Reveals Immediate Microglial Reaction to Implantation of Microelectrode through Extension of Processes. J. Neural. Eng. 2012, 9, 066001. [PubMed: 23075490]
38. Meunier CJ; Denison JD; McCarty GS; Sombers LA Interpreting Dynamic Interfacial Changes at Carbon Fiber Microelectrodes Using Electrochemical Impedance Spectroscopy. Langmuir 2020, 36, 4214–4223. [PubMed: 32216254]
39. Park Y; Chung TS; Lee G; Rogers JA Materials Chemistry of Neural Interface Technologies and Recent Advances in Three-Dimensional Systems. Chem. Rev. 2022, 122, 5277–5316. [PubMed: 34739219]
40. Kim DH; Viventi J; Amsden JJ; Xiao J; Vigeland L; Kim YS; Blanco JA; Panilaitis B; Frechette ES; Contreras D; Kaplan DL; Omenetto FG; Huang Y; Hwang KC; Zakin MR; Litt B; Rogers JA Dissolvable Films of Silk Fibroin for Ultrathin Conformal Bio-Integrated Electronics. Nat. Mater. 2010, 9, 511–517. [PubMed: 20400953]

41. Kaltenbrunner M; Sekitani T; Reeder J; Yokota T; Kuribara K; Tokuhara T; Drack M; Schwodiauer R; Graz I; Bauer-Gogonea S; Bauer S; Someya T An Ultra-Lightweight Design for Imperceptible Plastic Electronics. Nature 2013, 499, 458–463. [PubMed: 23887430]

42. Luan L; Wei X; Zhao Z; Siegel JJ; Potnis O; Tuppen CA; Lin S; Kazmi S; Fowler RA; Holloway S; Dunn AK; Chitwood RA; Xie C Ultraflexible Nanoelectronic Probes Form Reliable, Glial Scar-Free Neural Integration. Sci. Adv. 2017, 3, e1601966. [PubMed: 28246640]

43. Shi J; Fang Y Flexible and Implantable Microelectrodes for Chronically Stable Neural Interfaces. Adv. Mater. 2019, 31, e1804895. [PubMed: 30300442]

44. Wang C; Qi B; Lin M; Zhang Z; Makihata M; Liu B; Zhou S; Huang YH; Hu H; Gu Y; Chen Y; Lei Y; Lee T; Chien S; Jang KI; Kistler EB; Xu S Continuous Monitoring of Deep-Tissue Haemodynamics with Stretchable Ultrasonic Phased Arrays. Nat. Biomed. Eng. 2021, 5, 749–758. [PubMed: 34272524]

45. Jiang Y; Zhang Z; Wang YX; Li D; Coen CT; Hwaun E; Chen G; Wu HC; Zhong D; Niu S; Wang W; Saberi A; Lai JC; Wu Y; Wang Y; Trotsyuk AA; Loh KY; Shih CC; Xu W; Liang K; et al. Topological Supramolecular Network Enabled High-Conductivity, Stretchable Organic Bioelectronics. Science 2022, 375, 1411–1417. [PubMed: 35324282]

46. Gunasekera B; Saxena T; Bellamkonda R; Karumbaiah L Intracortical Recording Interfaces: Current Challenges to Chronic Recording Function. ACS Chem. Neurosci. 2015, 6, 68–83. [PubMed: 25587704]

47. Wen X; Wang B; Huang S; Liu TL; Lee MS; Chung PS; Chow YT; Huang IW; Monbouquette HG; Maidment NT; Chiou PY Flexible, Multifunctional Neural Probe with Liquid Metal Enabled, Ultra-Large Tunable Stiffness for Deep-Brain Chemical Sensing and Agent Delivery. Biosens. Bioelectron. 2019, 131, 37–45. [PubMed: 30818131]

48. Rogers JA; Lagally MG; Nuzzo RG Synthesis, Assembly and Applications of Semiconductor Nanomembranes. Nature 2011, 477, 45–53. [PubMed: 21886156]

49. Kim DH; Ahn JH; Choi WM; Kim HS; Kim TH; Song J; Huang YY; Liu Z; Lu C; Rogers JA Stretchable and Foldable Silicon Integrated Circuits. Science 2008, 320, 507–511. [PubMed: 18369106]

50. Cointe C; Laborde A; Nowak LG; Arvanitis DN; Bourrier D; Bergaud C; Maziz A Scalable Batch Fabrication of Ultrathin Flexible Neural Probes Using a Bioresorbable Silk Layer. Microsyst. Nanoeng. 2022, 8, 21. [PubMed: 35251687]

51. Chen H; Rim YS; Wang IC; Li C; Zhu B; Sun M; Goorsky MS; He X; Yang Y Quasi-Two-Dimensional Metal Oxide Semiconductors Based Ultrasensitive Potentiometric Biosensors. ACS Nano 2017, 11, 4710–4718. [PubMed: 28430412]

52. Angoa-Perez M; Kane MJ; Briggs DI; Herrera-Mundo N; Sykes CE; Francescutti DM; Kuhn DM Mice Genetically Depleted of Brain Serotonin Do Not Display a Depression-Like Behavioral Phenotype. ACS Chem. Neurosci. 2014, 5, 908–919. [PubMed: 25089765]

53. Ishikawa FN; Curreli M; Chang HK; Chen PC; Zhang R; Cote RJ; Thompson ME; Zhou C A Calibration Method for Nanowire Biosensors to Suppress Device-to-Device Variation. ACS Nano 2009, 3, 3969–3976. [PubMed: 19921812]

54. Aroonyadet N; Wang X; Song Y; Chen H; Cote RJ; Thompson ME; Datar RH; Zhou C Highly Scalable, Uniform, and Sensitive Biosensors Based on Top-Down Indium Oxide Nanoribbons and Electronic Enzyme-Linked Immunosorbent Assay. Nano Lett. 2015, 15, 1943–1951. [PubMed: 25636984]

55. Lu L; Gutruf P; Xia L; Bhatti DL; Wang X; Vazquez-Guardado A; Ning X; Shen X; Sang T; Ma R; Pakeltis G; Sobczak G; Zhang H; Seo DO; Xue M; Yin L; Chanda D; Sheng X; Bruchas MR; Rogers JA Wireless Optoelectronic Photometers for Monitoring Neuronal Dynamics in the Deep Brain. Proc. Natl. Acad. Sci. U. S. A. 2018, 115, E1374–E1383. [PubMed: 29378934]

56. Tringides CM; Vachicouras N; de Lazaro I; Wang H; Trouillet A; Seo BR; Elosegui-Artola A; Fallegger F; Shin Y; Casiraghi C; Kostarelos K; Lacour SP; Mooney DJ Viscoelastic Surface Electrode Arrays to Interface with Viscoelastic Tissues. Nat. Nanotechnol. 2021, 16, 1019–1029. [PubMed: 34140673]

57. Mathews TA; Fedele DE; Coppelli FM; Avila AM; Murphy DL; Andrews AM Gene Dose-Dependent Alterations in Extraneuronal Serotonin but Not Dopamine in Mice with Reduced

Serotonin Transporter Expression. J. Neurosci. Methods 2004, 140, 169–181. [PubMed: 15589347]

58. Yang H; Thompson AB; McIntosh BJ; Altieri SC; Andrews AM Physiologically Relevant Changes in Serotonin Resolved by Fast Microdialysis. ACS Chem. Neurosci. 2013, 4, 790–798. [PubMed: 23614776]
59. Yang H; Sampson MM; Senturk D; Andrews AM Sex- and SERT-Mediated Differences in Stimulated Serotonin Revealed by Fast Microdialysis. ACS Chem. Neurosci. 2015, 6, 1487–1501. [PubMed: 26167657]
60. Abdalla A; Atcherley CW; Pathirathna P; Samaranayake S; Qiang B; Pena E; Morgan SL; Heien ML; Hashemi P In Vivo Ambient Serotonin Measurements at Carbon-Fiber Microelectrodes. Anal. Chem. 2017, 89, 9703–9711. [PubMed: 28795565]
61. Ware T; Simon D; Liu C; Musa T; Vasudevan S; Sloan A; Keefer EW; Rennaker RL 2nd; Voit W. Thiol-Ene/Acrylate Substrates for Softening Intracortical Electrodes. J. Biomed. Mater. Res. B Appl. Biomater. 2014, 102, 1–11. [PubMed: 23666562]
62. Ware T; Simon D; Arreaga-Salas DE; Reeder J; Rennaker R; Keefer EW; Voit W Fabrication of Responsive, Softening Neural Interfaces. Adv. Funct. Mater. 2012, 22, 3470–3479.
63. Tien LW; Wu F; Tang-Schomer MD; Yoon E; Omenetto FG; Kaplan DL Silk as a Multifunctional Biomaterial Substrate for Reduced Glial Scarring around Brain-Penetrating Electrodes. Adv. Funct. Mater. 2013, 23, 3185–3193.
64. Obaid A; Wu Y-W; Hanna M; Jáidar O; Nix W; Ding J; Melosh N Ultra-Sensitive Measurement of Brain Penetration Mechanics and Blood Vessel Rupture with Microscale Probes. bioRxiv preprint 2020, DOI: 10.1101/2020.1109.1121.306498.
65. Ferguson BS; Hoggarth DA; Maliniak D; Ploense K; White RJ; Woodward N; Hsieh K; Bonham AJ; Eisenstein M; Kippin TE; Plaxco KW; Soh HT Real-Time, Aptamer-Based Tracking of Circulating Therapeutic Agents in Living Animals. Sci. Transl. Med. 2013, 5, 213ra165.
66. Dauphin-Ducharme P; Yang K; Arroyo-Curras N; Ploense KL; Zhang Y; Gerson J; Kurnik M; Kippin TE; Stojanovic MN; Plaxco KW Electrochemical Aptamer-Based Sensors for Improved Therapeutic Drug Monitoring and High-Precision, Feedback-Controlled Drug Delivery. ACS Sens. 2019, 4, 2832–2837. [PubMed: 31556293]
67. Hou H; Jin Y; Wei H; Ji W; Xue Y; Hu J; Zhang M; Jiang Y; Mao L A Generalizable and Noncovalent Strategy for Interfacing Aptamers with a Microelectrode for the Selective Sensing of Neurotransmitters in Vivo. Angew. Chem. Int. Ed. 2020, 59, 18996–19000.
68. Li X; Jin Y; Zhu F; Liu R; Jiang Y; Jiang Y; Mao L Electrochemical Conjugation of Aptamers on a Carbon Fiber Microelectrode Enables Highly Stable and Selective in Vivo Neurosensing. Angew. Chem. Int. Ed. 2022, 61, e202208121.

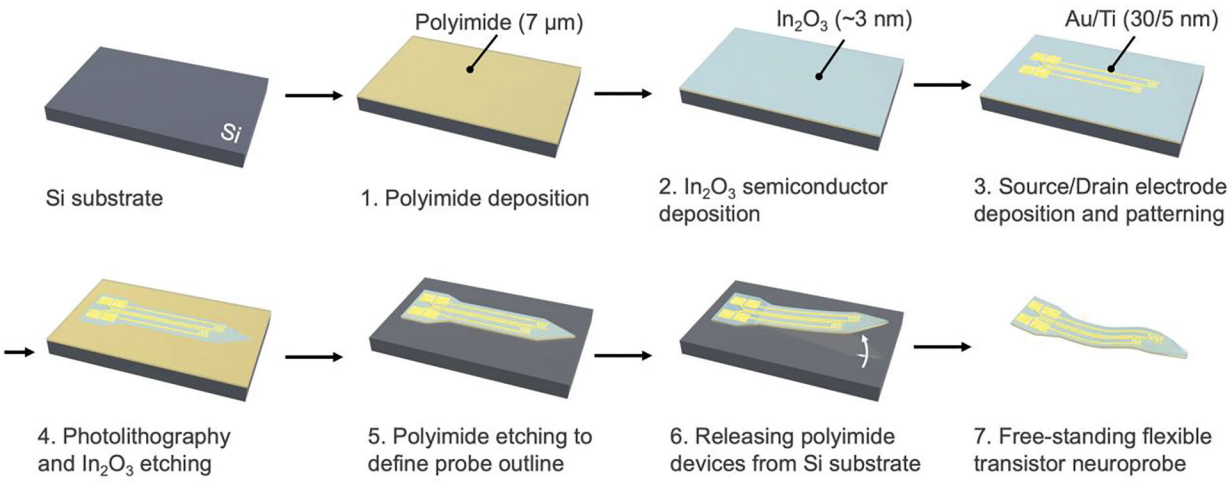

Figure 1. Schematic of the flexible neuroprobe fabrication process.

A polyimide film was deposited on a Si substrate (1), followed by the deposition of In_2O_3 (2). Source and drain electrodes were patterned by photolithography followed by metal evaporation of Au and Ti (3). To define the outline of the neuroprobe, a second lithography process was used followed by oxygen-plasma etching of In_2O_3 (4) and polyimide (5). Each fabricated polyimide device was released from the Si substrate using tweezers (6) to obtain individual flexible neuroprobes (7).

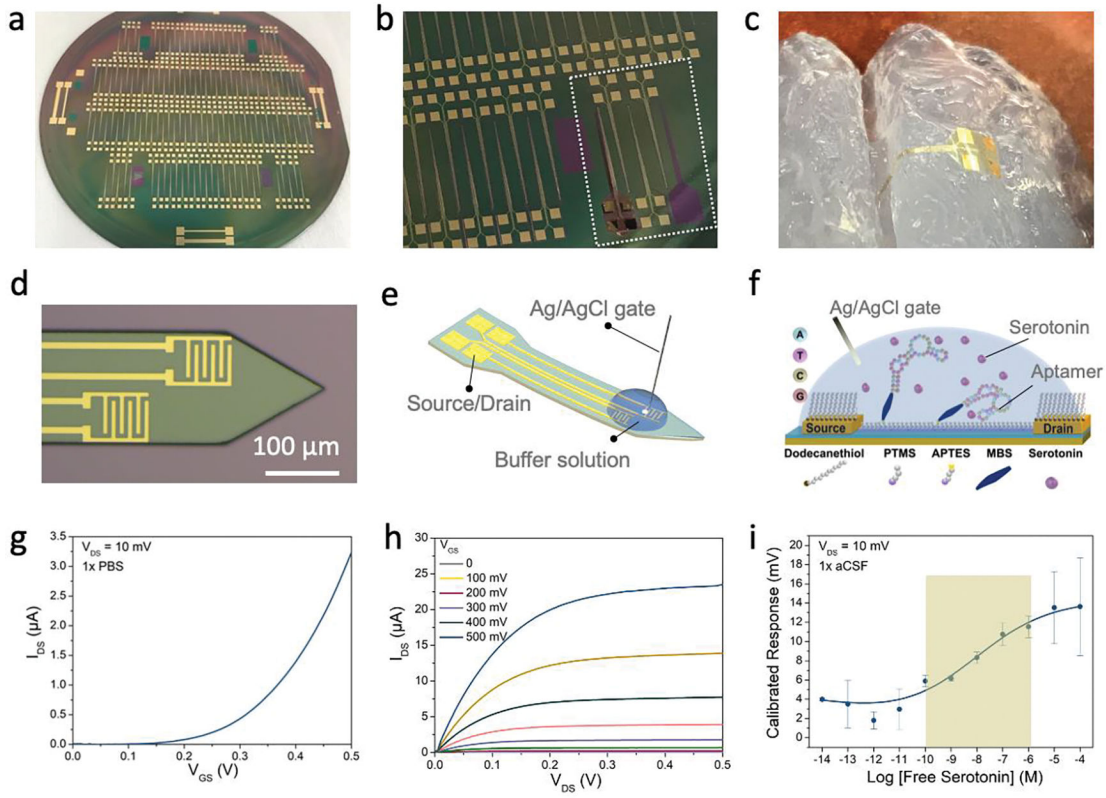

Figure 2. Serotonin sensing using aptamer-functionalized flexible neuroprobes.

(a) Photograph of 150 flexible probes fabricated on a 4” Si wafer. **(b)** Photograph of released probes on a Si substrate. As highlighted in the white box, the probe on the left has been partially released while the probe on the right has been completely released from the substrate. **(c)** Photograph of a flexible polyimide probe on a hydrogel matrix, which serves here as a brain mimic, showing the probe flexibility (tip width 150 µm). **(d)** Optical microscope image showing the tip of one neuroprobe with two field-effect transistors side-by-side. **(e)** Schematic of the measurement setup of a flexible neuroprobe, where a Ag/AgCl electrode was used to gate the FET through the buffer solution. **(f)** Schematic of the surface chemistry used to covalently functionalize aptamers onto the In_2O_3 surface. PTMS, trimethoxy(propyl)silane; APTMS, (3-aminopropyl)trimethoxysilane; MBS, 3-maleimidobenzoic acid *N*-hydroxysuccinimide ester. **(g,h)** Transfer and output curves, respectively, of a representative FET on a polyimide neuroprobe in phosphate buffered saline. PBS, phosphate buffered saline. **(i)** Sensing results for serotonin in artificial cerebrospinal fluid, where the highlighted box shows the physiological range of serotonin in the extracellular space. aCSF, artificial cerebrospinal fluid. Error bars are standard errors of the means of measurements from *N*=3 different probes.

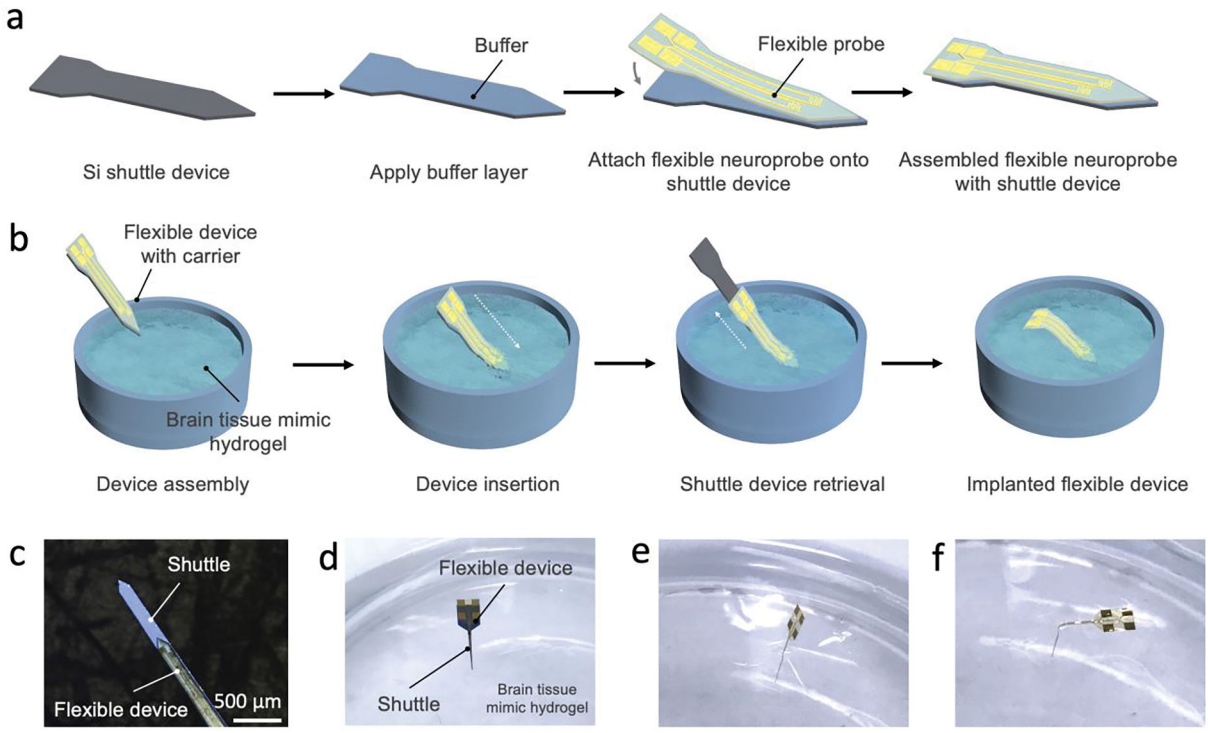

Figure 3. Implantation of a flexible neuroprobe into a brain-mimic hydrogel.

(a) Schematic illustration of device assembly before implantation. A flexible probe was attached to a Si shuttle *via* surface tension and aligned under a microscope. **(b)** Schematic illustration of flexible probe implantation using a Si probe as the shuttle device. The assembled device penetrates the hydrogel without buckling. After insertion, the buffer layer between the flexible probe and the Si shuttle device diffuses between the hydrogel. The edge surface tension is relieved, enabling the flexible probe to be separated from the Si shuttle. The shuttle is removed, leaving the flexible probe implanted in the hydrogel. **(c)** Optical microscope image of an assembled device, where the flexible probe is partially aligned to the Si shuttle device. Photographs of **(d)** an assembled device implanted into the hydrogel, and **(e, f)** a freestanding flexible probe implanted in the brain-mimic hydrogel.

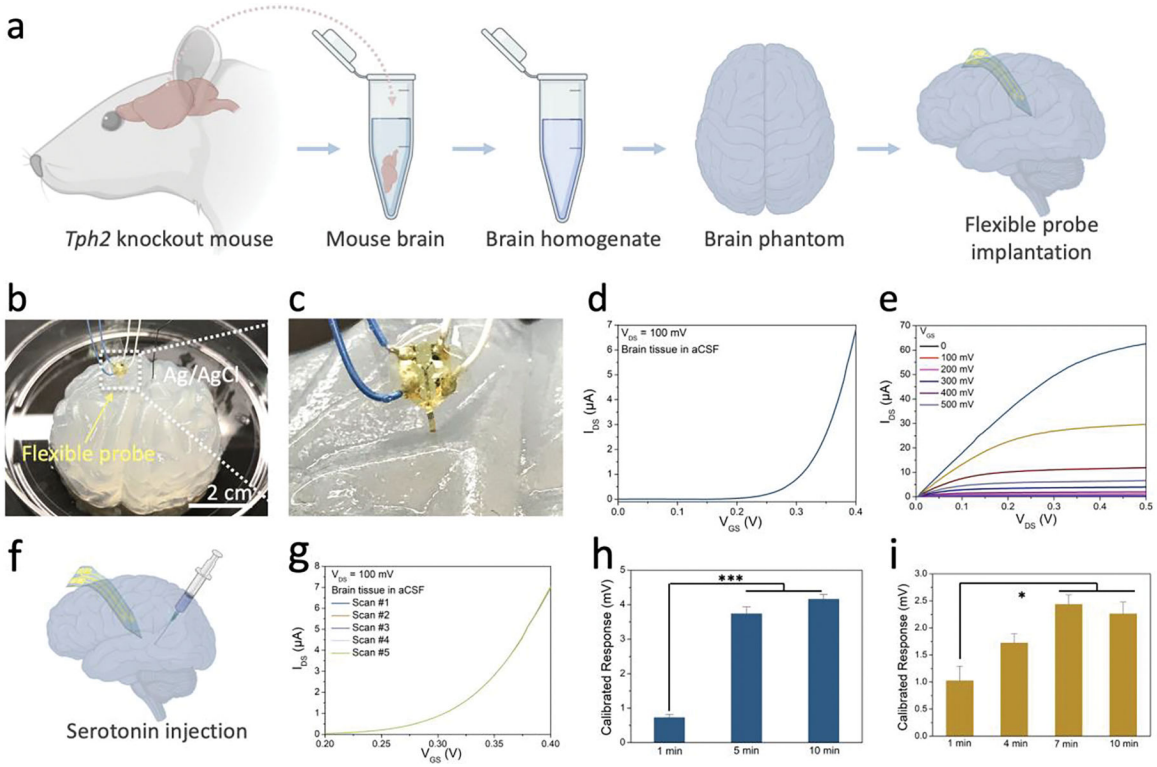

Figure 4. *Ex vivo* sensing of serotonin in a brain phantom.

(a) Schematic illustration of brain phantom preparation. Brains from *Tph2* null mice were removed and the tissue was homogenized in artificial cerebrospinal fluid (aCSF). The brain tissue homogenate was then mixed with 0.6% agarose gel in aCSF to make the brain-mimic for flexible probe implantation. **(b,c)** Photographs of an implanted flexible probe in the brain phantom, where a Ag/AgCl electrode was also implanted to apply a gate voltage. The source and drain electrodes were wired, sealed with epoxy, and connected to external measurement instrumentation. **(d)** Transfer characteristics of a representative field-effect transistor on a flexible probe after implantation in the brain phantom. **(e)** Output characteristics of a field-effect transistor on a flexible probe after implantation in the brain phantom. **(f)** Schematic illustration of serotonin injection using a syringe placed next to an implanted probe. **(g)** Five consecutive overlapping transfer sweeps of an implanted neuroprobe in the tissue-hydrogel brain-mimic before serotonin injection. **(h)** Calibrated responses of a representative neuroprobe after exposure to serotonin diffusing to the probe over time (100 nM final concentration). Error bars are standard errors of the means for N=5 sweeps. ***P<0.005 for 1 min *vs.* 5 and 10 min. **(i)** Calibrated responses from a different neuroprobe after exposure to 100 nM serotonin over time. Error bars are standard errors for N=5 sweeps. *P<0.05 for 1 min *vs.* 7 and 10 min.